

## **A Monte Carlo Computer Code to Calculate Radiation Dose from Syringes Containing Radioactive Substances**

S. Sherbini, W. Schadt, M. Thomas, H. Sadeghi Alavijeh, and A. Tripathi

*Howard University, Washington, DC*

*The absorbed dose to tissue surrounding a syringe containing technetium-99m is evaluated with a computer code using Monte Carlo photon-transport techniques. The syringe geometry is represented as a right circular cylinder. The cylindrical symmetry of the absorbed-dose distribution is assumed by calculating the absorbed dose in a volume region shaped like a circular annulus with a square cross section. The deposition of electron energy is assumed to take place at the point where the photon interacts. For a 5-ml syringe containing 3 ml of liquid, the absorbed dose at the midpoint of the liquid region and 0.5 mm from the outer syringe surface was 16.4 mrad per millicurie-minute. This is in good agreement with calculations and measurements reported in the literature. The accuracy of the program was tested by reproducing M. Berger's values of the specific absorbed fractions for point-isotropic sources in water. The code has been written in a flexible format. Any photon energy or mixture of photon energies, in any proportion, can be used as input to the program. The syringe dimensions and the volume of the liquid (source) region are variable input parameters. This code is intended to be used to produce absorbed-dose results a) for monoenergetic photons, b) for a variety of syringe sizes or source volumes, and c) to evaluate or optimize nonhomogeneous shielding materials such as lead, tungsten, uranium, and combinations of various materials.*

**J Nucl Med 20: 882-887, 1979**

Publications over the past several years have indicated a growing interest in the estimation of radiation exposure to technicians and others involved in nuclear medicine procedures. Of particular concern is the dose to the hands received during the preparation and administration by injection of radioactive substances before a scan or other tracer study. There has been an increasing suspicion that the dose rates from such procedures may be in excess of those allowed by regulations. Several studies have been conducted both to measure and also to calculate the dose to various parts of the hand using different emitters and syringe sizes.

Clayton (1) used thermoluminescent dosimeters (TLD) taped to the index finger and held against the syringe for 1 min. Takaku and Kida (2) used TLDs attached to tissue-equivalent fingers and irradiated for 1 day. Neil (3) held TLDs against syringes for 5 min. Anderson (4) attached TLDs to the fingers of technicians for 2-4 wk under normal working conditions. McEwan (5) taped TLDs around syringes and irradiated for several hours. Hušák (6) calculated the dose using specific gamma constants and tabulated "Gusev" functions. Henson (7) also calculated the dose using specific gamma constants, build-up factors, and the Loevinger function. Although the results of these measurements and calculations show general agreement, results differ in some instances by as much as a factor of six (1,2). Also, many of the data from

Received May 15, 1978; revision accepted Aug. 23, 1978.

For reprints contact: S. Sherbini, Nuclear Engineering Program, Howard University, Washington, DC 20059.

these studies cannot be compared directly because of differences such as syringe dimensions, size of active region, and conditions under which the measurements were performed. Calibration and dosimeter dimensions may also have had some effect on the results. The methods used in the theoretical dose calculations involve assumptions such as infinite media, build-up factors, and the use of special functions. Moreover, these methods become difficult to apply in cases involving nonhomogeneous media.

The purpose of the work described here is to develop a computer code that requires the minimum number of assumptions and that could be easily adapted to handle any combination of source-region size, source geometry, source type, and surrounding regions of interest.

#### PROCEDURE

The operation of the code is based on Monte Carlo techniques. These involve tracing the paths of a large number of photons from the points of generation within the syringe up to the point of complete absorption anywhere in the surrounding medium. Probability functions are used to select, at each phase of the photon's life, one of several possibilities determining its subsequent fate. Since the generation and interaction of photons within the system can be broken down into a series of fairly well-defined phases, the computer code has been written in sections, each reflecting one phase of the process. These sections are implemented in the code in the form of subroutines.

Initial system specifications are entered as input data in the main program. The data include dimensions of the active volume, energies and intensities of the photons to be considered, and the points at which the dose is to be evaluated. The total number of histories is also specified.

The first step in each photon history is the selection of the point of origin and initial direction of travel. This calculation is performed by subroutine SOURCE. The cylindrical coordinates of the point of generation are first selected using random numbers and are then converted to Cartesian coordinates. The active volume is assumed to be a right circular cylinder and the center of coordinates is located at the center of the base of the cylinder. The z-axis points along the cylinder axis. Throughout this paper, the symbol  $\xi$  will be used to represent a random number. If  $R$ ,  $\theta$ , and  $z$  are the cylindrical coordinates of the point of generation, then

$$\begin{aligned} R &= RI \times \sqrt{\xi_1}, \\ \theta &= 2\pi \times \xi_2, \text{ and} \\ Z &= ZA \times \xi_3, \end{aligned}$$

where  $RI$  and  $ZA$  are the radius and height of the active volume, respectively. From the coordinates, the Cartesian coordinates  $x$ ,  $y$ , and  $z$  are easily obtained. The direction cosines  $U$ ,  $V$ , and  $W$  for the initial photon path are then calculated. If  $\Omega$  and  $\phi$  specify the initial direction of the photon's path, where  $\Omega$  is measured from the  $z$ -axis and ranges from zero to  $\pi$ , and  $\phi$  is measured from the  $x$ -axis and ranges from zero to  $2\pi$ , then

$$\begin{aligned} \phi &= 2\pi \times \xi_4 \text{ and} \\ \Omega &= \arccos(\xi_5). \end{aligned}$$

Since the latter equation gives a range for  $\Omega$  of  $\pi/2$ , the angle is reflected with equal probability into the second quadrant. The direction cosines are then given by

$$\begin{aligned} U &= \sin \Omega \cos \phi, \\ V &= \sin \Omega \sin \phi, \text{ and} \\ W &= \cos \Omega. \end{aligned}$$

The next phase in following the photon's history is to select a path length, therefore giving a point of first interaction. The attenuation coefficients for the photon energy under consideration are determined by subroutine SECTN. The medium is assumed to have the attenuation properties of water, and the coefficients are obtained using the following equations (8):

$$\tau = \text{EXP}(6.74 - 3.24 \ln E),$$

where  $\tau$  is the photoelectric attenuation coefficient in  $\text{mm}^{-1}$ , and  $E$  is the photon energy in keV; and

$$\begin{aligned} \sigma &= 0.001(-\ln E + 23.7) \quad 0 < E \leq 25 \text{ keV} \\ &= 0.001(-2.755 \ln E + 29.36) \quad 25 < E \leq 85 \text{ keV} \\ &= 0.001(-4.142 \ln E + 35.55) \quad 85 < E \leq 200 \text{ keV} \end{aligned}$$

and

$$\mu = \tau + \sigma,$$

where  $\sigma$  is the Compton attenuation coefficient,  $\text{mm}^{-1}$ ,  $\mu$  is the total attenuation coefficient,  $\text{mm}^{-1}$ , and  $E$  is the photon energy in keV.

Note that the equations above handle photons of energy up to 200 keV. This is because the emitter of interest in this study is Tc-99m. Other energies can easily be accommodated by including equations for higher-energy photons and also for pair-production interactions if the photon energy is high enough.

Having determined the attenuation coefficients, the path length is calculated in the main program using the expression

$$S = -\frac{\ln \xi}{\mu}.$$

The coordinates of the point of interaction are therefore

$$\begin{aligned} X_1 &= X + S \times U, \\ Y_1 &= Y + S \times V, \text{ and} \\ Z_1 &= Z + S \times W. \end{aligned}$$

The type of interaction is selected by subroutine KIND as follows:

$$R = \frac{\sigma}{\mu}.$$

If  $R > \xi$ , the interaction is taken to be a Compton scattering; otherwise, the photon is considered to have been absorbed in a photoelectric process. The parameters of the interaction are calculated using one of two subroutines—COMPOT or PHOTO—depending upon whether the photon is scattered or absorbed. For a Compton scattering COMPOT evaluates the energies of the scattered photon and the Compton electron, as well as the angles of scattering. This is done as follows: A value of the scattering angle  $\theta$  is randomly chosen between 0 and  $\pi$ . The energy of the scattered photon is then calculated:

$$E_1 = \frac{E}{1 + \frac{E}{511}(1 - \cos \theta)}.$$

The Klein-Nishina equation for the differential scattering cross-section of unpolarized radiation (9) is used, together with the technique of sampling by rejection, to determine whether the chosen value of  $\theta$  should be accepted. If not, a new  $\theta$  is chosen randomly and the process repeated. Note that it was necessary to make an initial calculation of  $E_1$  because it appears as one of the terms in the Klein-Nishina equation. We concede that this method of selecting a value for  $\theta$  is not very sophisticated. However, one of the reasons that initially prompted its use was its simplicity. Future applications of this code will incorporate a more efficient application of the Klein-Nishina equation.

Once a value is chosen for  $\theta$ , the remaining scattering parameters are calculated. The azimuthal scattering angle  $\Phi$  is randomly chosen:

$$\Phi = 2\pi \times \xi,$$

and the energy of the Compton electron is found from

$$E_e = E - E_1.$$

The scattering angle for the electron is given by

$$\cot(\lambda) = \left(1 + \frac{E}{511}\right) \tan\left(\frac{\theta}{2}\right).$$

It should be noted here that although the angle  $\lambda$  is calculated, it was not used in the program executions reported in this paper because, for these runs, the assumption was made that the electron deposits all of its energy at the point of generation. The calculation of  $\lambda$  was included to allow for the possibility of removing this assumption should it become desirable to do so at a future time. The steps involved in this calculation are easily bypassed during execution of the program in order not to use unnecessary computer time.

If the interaction is a photoelectric absorption, subroutine PHOTO is called. This program supplies the energy of the photoelectron and the direction of electron emission. The energy is obtained quite simply from

$$E_e = E - 0.5 \text{ keV},$$

where 0.5 is taken to be the average binding energy of the electron. The direction of electron emission is determined by using sampling by rejection together with the photoelectric differential cross section (10) as the probability distribution function for the angle of emission. Again, the angle of emission was not used in the runs reported here because of the assumption of local energy deposition, but is available should this assumption be relaxed in future runs.

Regardless of the type of interaction occurring, the energy of the electron produced is added to energies previously deposited in the same volume element. Statistical parameters are also updated at this point.

Following a photoelectric interaction, the program returns to subroutine SOURCE to start a new history. If the interaction was a Compton scattering, subroutine NEWDIR is called. This subroutine determines the direction cosines of the scattered photon's path using the initial direction cosines and the scattering angles obtained from COMPOT. The equations used are standard equations from solid geometry (11). The scattered photon is followed in the same manner as was the original photon, and the process is repeated until the photon is absorbed or until its energy drops below 2 keV. In the latter case the photon is considered to behave as an electron of the same energy and its energy is deposited locally.

Throughout the program and within the subroutines, random numbers are generated as they are needed by a subroutine named SRAND. This is an IBM library subroutine available on the System 370 computer, on which the code was run. A flow diagram illustrating the logic of the computation procedure is shown in Fig. 1.

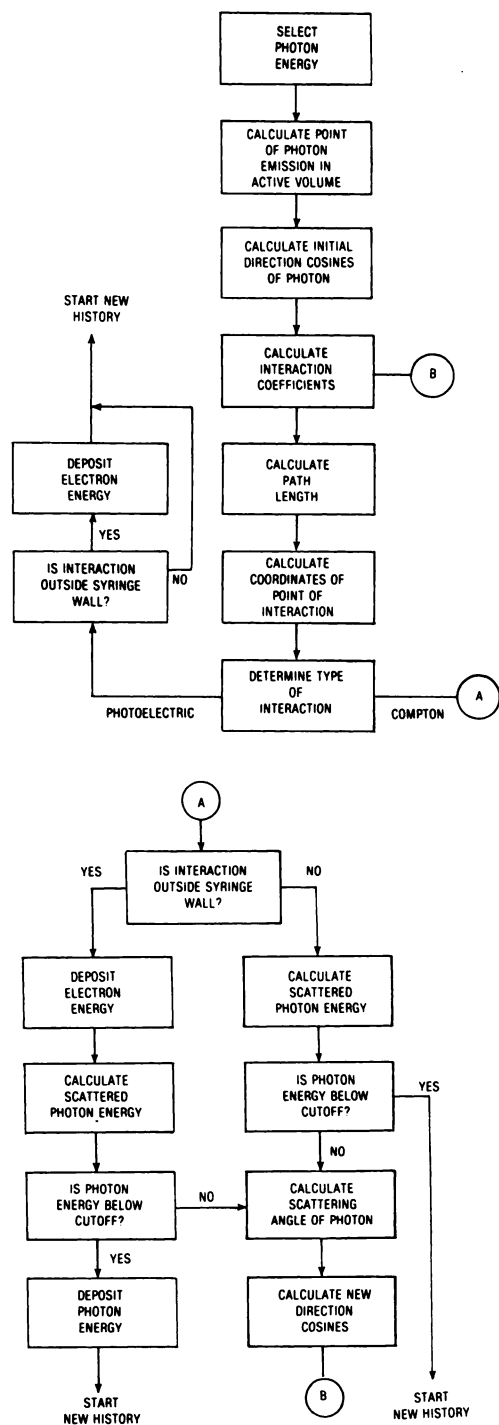


FIG. 1. Flow diagram showing steps involved in following history of photon starting from its emission in active region of syringe.

RESULTS

Before the main program was run, each subroutine was tested individually. This was done by writing programs designed to verify proper functioning of the subroutines. Values generated by these tests

were compared with corresponding values in the literature or were subjected to statistical analysis whenever appropriate. The next step was to verify the proper operation of the main program, and to this end it was decided to generate published and accepted data involving photon transport. Berger's data (12) on specific absorbed fractions from a point source in an infinite medium were selected. To simulate a point source the syringe dimensions were set to 1-mm radius and 1-mm active length. The test was run twice, first with the medium subdivided into concentric spherical shells with their center coinciding with the center of coordinates, and second by subdividing the regions surrounding the source into concentric annular rings centered around the z-axis of coordinates. Both runs gave results that corresponded closely with Berger's data. The second run closely approximates the geometry used with full-sized syringes, and the results are shown in Table 1. The total number of histories was 360,000. The distances shown are measured from the z axis to the center of each annular region. These regions have square cross sections of 2-mm sides, except the annulus at 20 mm, which has a height of 2 mm and a radial width of 1 mm. The photon energies were fixed at 100 keV. The specific absorbed fraction was calculated using the equation

$$\phi(x) = \frac{E(x)}{ME(0)},$$

where  $E(x)$  is the energy deposited in the annulus at distance  $x$ ;  $E(0)$  is the total energy emitted by the source;  $M$  is the mass of the medium within the annulus; and  $E(0) = 100 \times 3.6 \times 10^5$  keV.

The code was next run for a full-sized syringe: 5 ml with a 3-ml active volume. The inner- and outer-wall radii were 0.593 cm and 0.642 cm, respectively. The plastic wall was assumed to have the same interaction properties as water and was assumed to be surrounded by an infinite water medium. The total number of histories considered in the run was

Code results		Relative standard deviation (%)	Berger's data	
X(cm)	$\phi(x)$		X(cm)	$\phi(x)$
0.7	4.93E-03	3.2	0.8	3.59E-03
2.0	6.50E-04	4.9	2.0	6.63E-04
2.9	3.21E-04	4.2	3.0	3.22E-04
3.9	2.19E-04	4.5	4.0	1.93E-04
4.9	1.45E-04	4.9	5.0	1.30E-04
5.9	9.31E-05	5.9	6.0	9.29E-05
7.9	5.41E-05	6.6	8.0	5.33E-05
9.9	3.10E-05	7.5	10.0	3.34E-05
11.9	2.16E-05	7.8	12.0	2.10E-05

**TABLE 2. DOSES AT THE CENTER OF THE ACTIVE VOLUME mrad/mCi-min**

R(cm)	Dose	Relative standard deviation (%)
0.05	16.42	3.54
1.36	2.33	5.79
2.26	1.34	4.18
4.26	0.54	5.36
6.26	0.27	6.62
8.26	0.14	8.17
10.26	0.10	8.13

**TABLE 3. DOSES 0.1 CM FROM END OF ACTIVE VOLUME mrad/mCi-min**

R(cm)	Dose	Relative standard deviation (%)
0.05	11.14	4.41
1.36	2.25	6.19
2.26	1.08	4.71
4.26	0.50	5.94
6.26	0.26	6.48
8.26	0.13	8.28
10.26	0.12	7.83

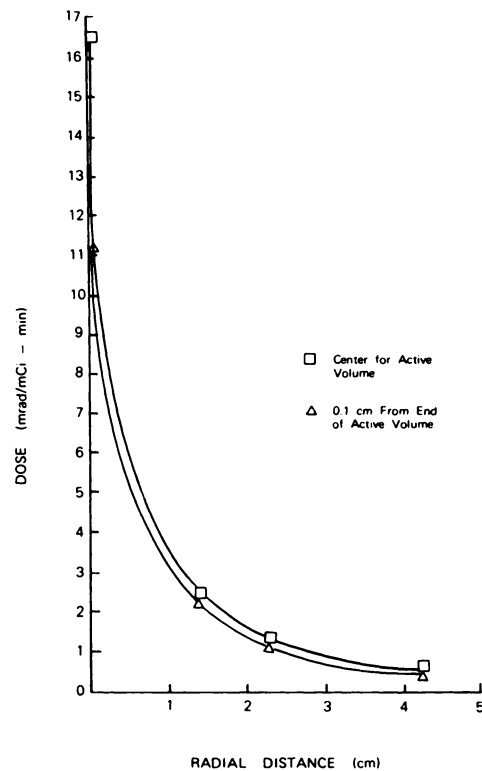


FIG. 2. Radial dose distribution from outer surface of syringe up to 4.26 cm from surface at two axial locations.

360,000. The energies and intensities of the photons were those for Tc-99m obtained from MIRD Pamphlet No. 10 (13). The dose was determined at five axial locations along the active volume, one at the center, two at the ends, and one between the center and each end. At each of these five axial positions the dose was obtained at different distances from the outer syringe surface, starting at the wall. Tables 2-5 show some of the results. The annuli over which the doses were accumulated were of square section with a 0.2-cm side, except the innermost two, which had rectangular sections with a height of 0.2 cm and a radial thickness of 0.1 cm. Tables 2 and 3 show the radial dose distribution at the center and bottom of the active volume, respectively. Tables 4 and 5 show the axial dose distribution along the active volume at the surface and at a mean distance of 4.26 cm from the surface, respectively. The radial dose distributions given in Tables 2 and 3 are shown in Fig. 2, and the axial distributions given in Tables 4 and 5 are shown in Fig. 3.

The results shown are found to compare well with those in the literature. The dose at the surface in the center of the active volume is 16.42 mrad/mCi-min, compared to 13 mrad/mCi-min calculated by Hušák (6) for a 2-ml syringe, and 20 mrad/mCi-min calculated by Henson (7) for a 5-ml syringe. This dose is also close to, though somewhat higher than, measured values reported in the literature. Thus, Clayton (1) measured 14.8 mrad/mCi-min for

**TABLE 4. DOSES 0.05 CM FROM OUTER SURFACE OF SYRINGE mrad/mCi-min**

Z(cm)	Dose	Relative standard deviation (%)
0.1	11.14	4.41
0.73	14.97	3.72
1.36	16.42	3.54
1.99	15.61	3.66
2.62	9.95	4.50

**TABLE 5. DOSES 4.26 CM FROM OUTER SURFACE OF SYRINGE mrad/mCi-min**

Z(cm)	Dose	Relative standard deviation (%)
0.1	0.50	5.94
0.73	0.54	5.65
1.36	0.54	5.36
1.99	0.52	5.45
2.62	0.45	6.18

a 1-ml active volume; Neil (3) obtained 10.5 mrad/mCi-min from 10 mCi of Tc-99m in a syringe of unspecified volume; McEwan (5) measured 12 mrad/mCi-min for a 3-ml active volume; and Anderson (4) obtained 7 mrad/mCi-min. This last result

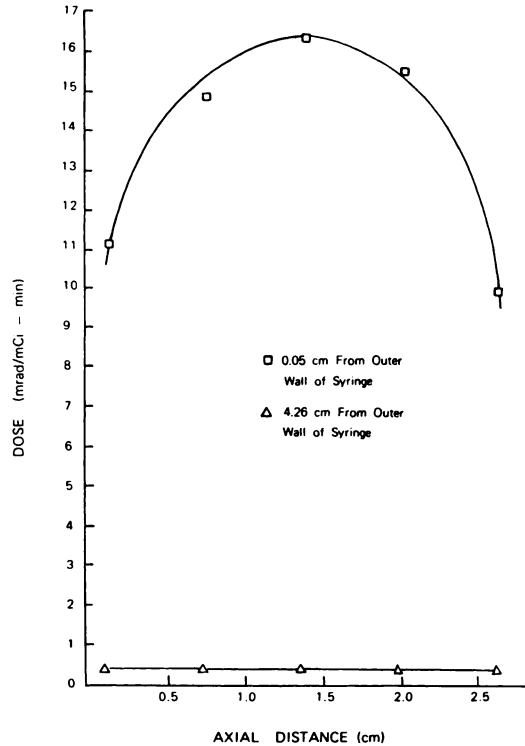


**FIG. 3.** Axial dose distribution along length of the active volume at the outer surface of syringe and at 4.26 cm from surface.

cannot be compared directly, however, because it represents the average dose received over several weeks by technicians performing a variety of functions related to nuclear medicine procedures.

#### DISCUSSION

The basic assumption incorporated in the code is that the energy of the electrons generated as a result of photon interactions is deposited at the site of interaction. The radionuclide considered in this study is Tc-99m, and the highest electron energy expected to be generated in any interaction is about 140 keV. The range of such an electron in water is approximately 0.24 mm. Since the regions over which the doses were integrated had linear dimensions of at least 1 mm, the assumption of local energy deposition seems justified. However, the code has been written in such a way that the relaxation of this assumption would require only minor modifications to the main program. One of the stud-

ies currently being contemplated is use of the code to study the effects of secondary electrons generated in the syringe walls (or in shields) on the dose at the surface of the syringe. This question is of interest because dose measurements reported in the literature in which calibration procedures were mentioned have used TLDs calibrated in Co-60 gamma fields. It is possible that the response of the dosimeters to low-energy electrons is such as to result in underestimating this contribution from secondary electrons. An underestimation of the dose at the surface of the syringe may also have occurred because of the fairly large dimensions of the dosimeters used, in comparison with the ranges of these low-energy secondary electrons.

#### REFERENCES

1. CLAYTON RS, WHITE JE, BRIEDEN M, et al: Skin exposure from handling syringes containing radioactive isotopes. *Am J Roentgenol* 105: 897-899, 1969
2. TAKAKU Y, KIDA T: Radiation dose to the skin and bone of the fingers from handling radioisotopes in a syringe. *Health Phy* 22: 295-297, 1972
3. NEIL CM: The question of radiation exposure to the hand from handling <sup>99m</sup>Tc. *J Nucl Med* 10: 732-734, 1969
4. ANDERSON DW, RICHTER CW, FICKEN VJ, et al: Use of thermoluminescent dosimeters for measurement of dose to the hands of nuclear medicine technicians. *J Nucl Med* 13: 627-629, 1972
5. McEWAN AC: Radiation doses in the handling of short-lived radionuclides. *Brit J Radiol* 42: 396, 1969
6. HUSAK V: Exposure rate at the surface of syringes containing radioactive material. *J Nucl Med* 12: 574-575, 1971
7. HENSON PW: Radiation dose to the skin in contact with unshielded syringes containing radioactive substances. *Brit J Radiol* 46: 972-977, 1973
8. HUBBELL, JH: Photon Cross-Sections, Attenuation Coefficients, and Energy Absorption Coefficients from 10 keV to 100 geV. U.S. Dept. of Commerce, NSRDS-NBS 29, 1969
9. EVANS RD: *The Atomic Nucleus*. New York, McGraw-Hill Book Co., 1969, pp 632-692
10. SHAFROTH SM: *Scintillation Spectroscopy of Gamma Radiation*, vol. 1, New York, Gordon and Breach Science Publishers, 1967, pp 274-277
11. CARTER LL, CASHWELL, ED: Particle-Transport Simulation with the Monte Carlo Method. Technical Inf. Cent., Off. Pub. Affairs, U.S. ERDA, TID-26607, 1975
12. BERGER MJ: Energy deposition in water by photons from point isotropic sources. *J Nucl Med* 9 (Suppl No. 1): 15, 1968
13. DILLMAN LT, VON DER LAGE FC: Radioactive decay schemes and nuclear parameters for use in radiation-dose estimation. NM/Mird pamphlet No. 10. New York, The Society of Nuclear Medicine